THE JOURNAL OF BIOLOGICAL CHEMISTRY VOL. 285, NO. 2, pp. 835–844, January 8, 2010

⌘ *Author's Choice*

N Terminus Is Key to the Dominant Negative Suppression of Ca_V2 Calcium Channels

IMPLICATIONS FOR EPISODIC ATAXIA TYPE 2[*][S]

Received for publication, September 10, 2009, and in revised form, October 27, 2009 Published, JBC Papers in Press, November 10, 2009, DOI 10.1074/jbc.M109.065045

Karen M. Page[1], **Fay Heblich**[1], **Wojciech Margas**[1], **Wendy S. Pratt, Manuela Nieto-Rostro, Kanchan Chaggar, Kieran Sandhu, Anthony Davies, and Annette C. Dolphin**[2]

From the Department of Neuroscience, Physiology, and Pharmacology, University College London, Gower Street, London WC1E 6BT, United Kingdom

Expression of the calcium channels $Ca_V2.1$ and $Ca_V2.2$ is markedly suppressed by co-expression with truncated constructs containing Domain I. This is the basis for the phenomenon of dominant negative suppression observed for many of the episodic ataxia type 2 mutations in $Ca_V2.1$ that predict truncated channels. The process of dominant negative suppression has been shown previously to stem from interaction between the full-length and truncated channels and to result in downstream consequences of the unfolded protein response and endoplasmic reticulum-associated protein degradation. We have now identified the specific domain that triggers this effect. For both $Ca_V2.1$ and $Ca_V2.2$, the minimum construct producing suppression was the cytoplasmic N terminus. Suppression was enhanced by tethering the N terminus to the membrane with a CAA*X* motif. The 11-amino acid motif (including Arg^{52} and Arg^{54}) within the N terminus, which we have previously shown to be required for G protein modulation, is also essential for dominant negative suppression. Suppression is prevented by addition of an N-terminal tag (XFP) to the full-length and truncated constructs. We further show that suppression of $Ca_V2.2$ currents by the N terminus-CAA*X* construct is accompanied by a reduction in $Ca_V2.2$ protein level, and this is also prevented by mutation of Arg^{52} and Arg^{54} to Ala in the truncated construct. Taken together, our evidence indicates that both the extreme N terminus and the Arg^{52}, Arg^{54} motif are involved in the processes underlying dominant negative suppression.

Voltage-gated calcium (Ca_V)[3] channels are required for a number of essential physiological processes; in particular, they are essential for many neuronal functions, including neurotransmitter release (for review, see Ref. 1). They are heteromeric complexes consisting of the pore-forming $Ca_V\alpha1$ subunit together (except in the case of the Ca_V3 channels) with an accessory β and $\alpha_2\delta$ subunit. The $Ca_V\alpha1$ subunit consists of four homologous domains (I–IV), each consisting of six transmembrane (TM) segments (see Fig. 1*A*). The domains are linked by intracellular loops and have intracellular N and C termini. Ten mammalian $\alpha1$ subunit genes have been cloned and divided into three subfamilies Ca_V1–3 (2).

Mutations of calcium channel $\alpha1$ subunits can contribute to a number of pathological states (3). In particular, mutations in the *CACAN1A* gene encoding $Ca_V2.1$ result in familial hemiplegic migraine and episodic ataxia type 2 (4). Many of the episodic ataxia type 2 mutations in $Ca_V2.1$ predict truncated forms of this channel, although missense mutations are also found (4–7). This disease is dominant, and thus there is one wild-type (WT) allele and one mutant allele, both of which are likely to be expressed, although nonsense-mediated decay would reduce the expression of some mutant alleles (8). In many cases, the mutant channels, as well as either being nonfunctional or having reduced functionality, are dominant negative, in that they also suppress the function of the WT channel (9–11).

In our initial study on truncated $Ca_V\alpha1$ subunits, we found that truncated constructs containing Domain I suppressed $Ca_V2.2$ currents and reduced the level of full-length $Ca_V2.2$ protein (12). We then showed that for both $Ca_V2.2$ and $Ca_V2.1$, this suppression required interaction between the full-length and the mutant construct (9). In this study, we also examined the effect of a two-domain construct predicted by an episodic ataxia type 2 mutation (9). We and others have also identified previously that the suppressive mechanism involves a reduction in protein synthesis resulting from the unfolded protein response (9) and an acceleration of proteasome-mediated decay (10).

Here, we have dissected the determinants required for suppression, which has increased our understanding of the mechanisms involved in the pathophysiology of episodic ataxia type 2. We find that the interaction between a truncated construct and a related full-length channel, identified previously (9), requires the presence of the N terminus on either or both of the full-length or the truncated channels. We also show that the N terminus of $Ca_V2.2$ or $Ca_V2.1$ alone is sufficient to suppress expression of the full-length channel. Suppression can be prevented by incorporation of a bulky tag on the N terminus or by removal of part of the N terminus. We further identify the

* This work was supported by Wellcome Trust Grant 077883 and Medical Research Coucil Grant G0700368.
⌘ *Author's Choice*—Final version full access.
[S] The on-line version of this article (available at http://www.jbc.org) contains supplemental "Methods," "Results," Table 1, Fig. 1, and additional references.
[1] These authors contributed equally to this work.
[2] To whom correspondence should be addressed. Tel.: 44-2076793276; Fax: 44-2076790042; E-mail: a.dolphin@ucl.ac.uk.
[3] The abbreviations used are: Ca_V channel, voltage-gated calcium channel; ANOVA, analysis of variance; BisTris, 2-[bis(2-hydroxyethyl)amino]-2-(hydroxymethyl)propane-1,3-diol; DMEM, Dulbecco's modified Eagle's medium; Dom, Domain; DRG, dorsal root ganglion; GFP, green fluorescent protein; S1–S4, segments S1 through S4; TM, transmembrane; WT, wild type; YFP, yellow fluorescent protein; XFP, any of the members of the GFP family.

motifs within the N terminus that are essential for suppression to occur and show that suppression can also be induced of endogenous channels in neurons.

EXPERIMENTAL PROCEDURES

Full-length, Mutant, and Truncated Ca_V Constructs—The following cDNAs were used: $Ca_V2.2$ (GenBank Accession number D14157), $\alpha_2\delta$-1 (GenBank Accession number M86621), $\alpha_2\delta$-2 (13), β1b (14), $Ca_v2.1$ (GenBank Accession number M64373), Kir2.1-AAA (15), and GFP-mut3b (16) in pMT2. The $Ca_V2.2$-Dom I and YFP-$Ca_V2.2$ constructs (12) and the Δ1–55 $Ca_V2.2$ truncation (17) have been described previously. Other constructs were made by standard techniques and verified by automated sequencing. They were: $Ca_v2.2$ N terminus (residues 1–95), $Ca_v2.1$ N terminus (residues 1–100), $Ca_V2.2$-Dom I-4TMs (residues 1–225 plus a C-terminal myc-His_6 tag), $Ca_V2.2$-Dom I-4TMs no charges (residues 1–225, with all charged residues in S1, S2, S3 and S4 replaced by the noncharged residues: valine, leucine, or isoleucine), $Ca_V2.2$-DomI-4TMs no charges-C110S, $Ca_V2.2$ Δ2–91 with an N-terminal SS motif to create a construct starting MSSTEW, $Ca_V2.2$-Dom I Δ2–91 and $Ca_V2.2$-Dom I Δ1–55. When a CAA*X* motif was added, this was the C-terminal 10 amino acids of H-Ras (GCMSCKCVLS). It was added to the C terminus of GFP-mut3b, $Ca_V2.2$ N terminus (residues 1–95), $Ca_V2.2$ N terminus containing the R52A/R54A mutation, $Ca_V2.2$ N terminus (Δ2–42), $Ca_V2.1$ N terminus (residues 1–100), and $Ca_V2.1$ N terminus R57A/R59A. These were all subcloned into an in-frame XhoI site of the CAA*X* pMT2 vector, which then creates an additional arginine residue between the construct and CAA*X* motif.

Cell Culture and Heterologous Expression—COS-7 cells were cultured as described previously (18). The tsA-201 cells were cultured in a medium consisting of Dulbecco's modified Eagle's medium (DMEM), 10% fetal bovine serum, 1% Glutamax, 100 units/ml penicillin, and 100 μg/ml streptomycin (Invitrogen). Cells were transfected using FuGENE 6 (Roche Diagnostics). The cDNAs (all at 1 μg/μl) for $Ca_V\alpha1$ subunits, truncated domain constructs, $\alpha_2\delta$-1 or $\alpha_2\delta$-2, β1b, and GFP, when used as a reporter of transfected cells, were mixed in a ratio of 3:1.5:2:1:0.2, unless stated otherwise. When particular subunits were not used, the volume was made up with water or blank vector, or the volume of transfection reagent was reduced, all with equivalent results.

Dorsal root ganglion (DRG) neurons isolated from Sprague-Dawley rats (175–250 g) in ice-cold Hanks' balanced salt solution (Invitrogen) were transferred to DMEM nutrient mixture F-12 (DMEM/F12) containing 0.4 mg/ml trypsin, 0.6 mg/ml collagenase type 1 (both from Worthington Biochemical Corp.), and 100 units/ml DNase (Invitrogen), saturated with 95% O_2/5% CO_2, and incubated for 1 h at 37 °C. The neurons were washed in DMEM/F12 supplemented with 10% fetal bovine serum, 1% penicillin-streptomycin, and 1% Glutamax (10% DMEM). Neurons were dissociated by vigorous shaking, centrifuged twice for 9 min at 800 × *g*, and the pellet was resuspended in 200 μl of Amaxa rat neuron nucleofector solution (Lonza Cologne AG, Cologne, Germany). Suspended neurons were mixed with cDNA for the truncated domain constructs (40 ng/μl) and YFP (20 ng/μl) DNA and transfected with nucleofector program O-003 following the manufacturer's instructions. The effect of the constructs was compared with DRG neurons expressing only YFP cDNA. The transfection reagent was neutralized with 500 μl of 10% DMEM supplemented with 50 ng/ml nerve growth factor. Neurons from each group were plated on poly-L-lysine (0.5 mg/ml)-coated 22-mm coverslips (BDH), placed in 35-mm polystyrene tissue culture dishes for 2 h to settle, flooded with 10% DMEM supplemented with 50 ng/ml nerve growth factor, and cultured for 3–4 days at 37 °C. Prior to experiments, the numerous neurite processes were eliminated by replating to improve voltage-clamp recording. Culture medium was removed, and cells were incubated for 5 min at 37 °C in 1 ml of 10% DMEM containing 0.2% type 1 collagenase. The enzymatic reaction was stopped with 1 ml of 10% DMEM, and the neurons were triturated and spun for 9 min at 800 × *g*. The pellet was resuspended in 300 μl of 10% DMEM, and the cells from each group were plated on poly-L-lysine-coated coverslips and left to recover for at least 2 h at 37 °C before recording.

Xenopus oocytes were prepared, injected, and utilized for electrophysiology as described previously (17), with the following exceptions. Plasmid cDNAs for the different calcium channel subunits $\alpha1$, $\alpha_2\delta$, β1b, and truncated or mutated domains and other constructs were mixed in 2:1:2:2 ratios at 1 μg/μl, unless stated otherwise, and 9 nl was injected intranuclearly, after 2-fold dilution of the cDNA mixes. When the truncated domain was not included it was replaced by an equivalent volume of empty vector, water, or a cDNA for a nonfunctional transmembrane protein, Kir-AAA (15) with equivalent results.

Electrophysiology—For tsA-201 cells, the patch pipette solution contained 140 mM cesium aspartate, 5 mM EGTA, 2 mM $MgCl_2$, 0.1 mM $CaCl_2$, 2 mM K_2ATP, 10 mM Hepes, pH 7.2, 310 mOsm with sucrose. The external solution contained 150 mM tetraethylammonium bromide, 3 mM KCl, 1.0 mM $NaHCO_3$, 1.0 mM $MgCl_2$, 10 mM Hepes, 4 mM glucose, 1 mM $BaCl_2$, pH 7.4, 320 mOsM with sucrose. For DRGs, the patch pipette solution contained 140 mM cesium aspartate, 10 mM EGTA, 2 mM $MgCl_2$, 5 mM K_2ATP, 10 mM Hepes, pH 7.2, 310 mOsm with sucrose. The external solution was identical to that described above, except 10 mM $BaCl_2$ was used, and 1 μM tetrodotoxin was included in the medium to suppress voltage-gated Na^+ currents. I_{Ba} was recorded using an Axopatch 1D amplifier (Axon Instruments, Molecular Devices, Sunnyvale CA), and data were filtered at 2 kHz and digitized at 10 kHz. Analysis was performed using pClamp9 (Axon) and Origin 7 (Microcal Origin, Northampton, MA). Current records are shown following leak and residual capacitance current subtraction (P/4 protocol). Incompletely subtracted capacitative transients have been truncated in traces shown. Recordings in *Xenopus* oocytes were performed as described (19), and all recordings were performed 48–60 h after injection for $Ca_V2.2$ and 72–80 h after injection for $Ca_V2.1$. The Ba^{2+} concentration was 10 mM, unless stated otherwise. When stated, current-voltage (*I-V*) plots were fit with a modified Boltzmann equation as described, for determination of the voltage for 50% activation (19).

Western Blotting and Calcium Channel Subunit Quantification—COS-7 cells were processed for SDS-PAGE as described (12). Samples (50 μg of cell lysate protein/lane) were separated using Novex 4–12% Tris-glycine or 4–12% BisTris

NuPAGE gels (Invitrogen) and transferred electrophoretically to polyvinylidene fluoride membranes. The membranes were blocked with 3% bovine serum albumin and 0.02% Tween 20 and then incubated overnight at room temperature with the relevant primary antibody: 1:1000 dilution of anti-$Ca_v2.2$ (12). Detection was performed either with a 1:1000 dilution of goat anti-rabbit (or anti-mouse) IgG-horseradish peroxidase conjugate (Bio-Rad) and ECL Plus (Amersham Biosciences), or with a 1:1000 dilution of goat anti-rabbit IgG-Cy5 conjugate (Amersham Pharmacia Biotech), all in conjunction with a Typhoon 9410 Variable Mode Imager (Amersham Pharmacia Biotech), set in chemiluminescence or fluorescence mode, respectively. Protein bands were quantified using ImageQuant 5.2. The same amount of total protein was loaded for all samples on a gel for accurate comparison between lanes.

RESULTS

To extend our studies on the suppression of $Ca_V2.x$ channels by truncated domains containing Domain I (Fig. 1*A*) (9, 12), in terms of the specific truncated domain involved, we first mutated various structural motifs in Domain I and expressed the resultant constructs to narrow down the element(s) responsible for the suppression. We have used a number of different expression systems and methods to ensure that our results are able to generalize beyond a single system. Key experiments have been reproduced by more than one method.

Which Structural Elements within Domain I of Ca_V2 Channels Are Required for Suppression?—$Ca_V2.2$-Dom I alone produced ~90% suppression of $Ca_V2.2$ currents in *Xenopus* oocytes (Fig. 1, *B* and *C*). $Ca_V2.2$-Dom I was previously found to be more effective than $Ca_V2.2$-Dom I-II to inhibit $Ca_V2.2$ currents (12). We then found that a construct consisting of the N terminus and the first four TM segments (S1–S4) of $Ca_V2.2$ ($Ca_V2.2$-Dom I-4TMs) was as effective as $Ca_V2.2$-Dom I, $Ca_V2.2$ I_{Ba} being reduced to 13% of control (Fig. 1, *B* and *C*). A conserved set of structural motifs in this region of $Ca_V2.2$-Dom I is the charged amino acids in TM segments S1–S4, which might mediate inappropriate interaction between the full-length and truncated channel. However, mutation of all charged amino acids in the TM segments S1, S2, S3, and S4 to hydrophobic residues, within the truncated $Ca_V2.2$-Dom I-4TMs construct, did not significantly affect the ability of this construct to suppress $Ca_V2.2$ currents (Fig. 1, *B* and *C*). A second potential source of interaction is the conserved cysteines (in S1 and S2) which might form disulfide bonds with the full-length WT channel. However, when the cysteine in S1 (Cys^{110}) was also mutated to serine to form $Ca_V2.2$-Dom I-4TMs (no charges, C110S), suppression of I_{Ba} was again undiminished (Fig. 1, *B* and *C*).

Role of the N Terminus of $Ca_V2.2$ in Dominant Negative Suppression—We then surmised that the cytoplasmic N terminus might contain structural elements involved in suppression. To examine the role of the N terminus, we utilized truncated and full-length constructs of $Ca_V2.2$, in which either or both were engineered to contain N-terminal deletions. We have previously shown that Δ1–55 $Ca_V2.2$ produced functional channels (17).

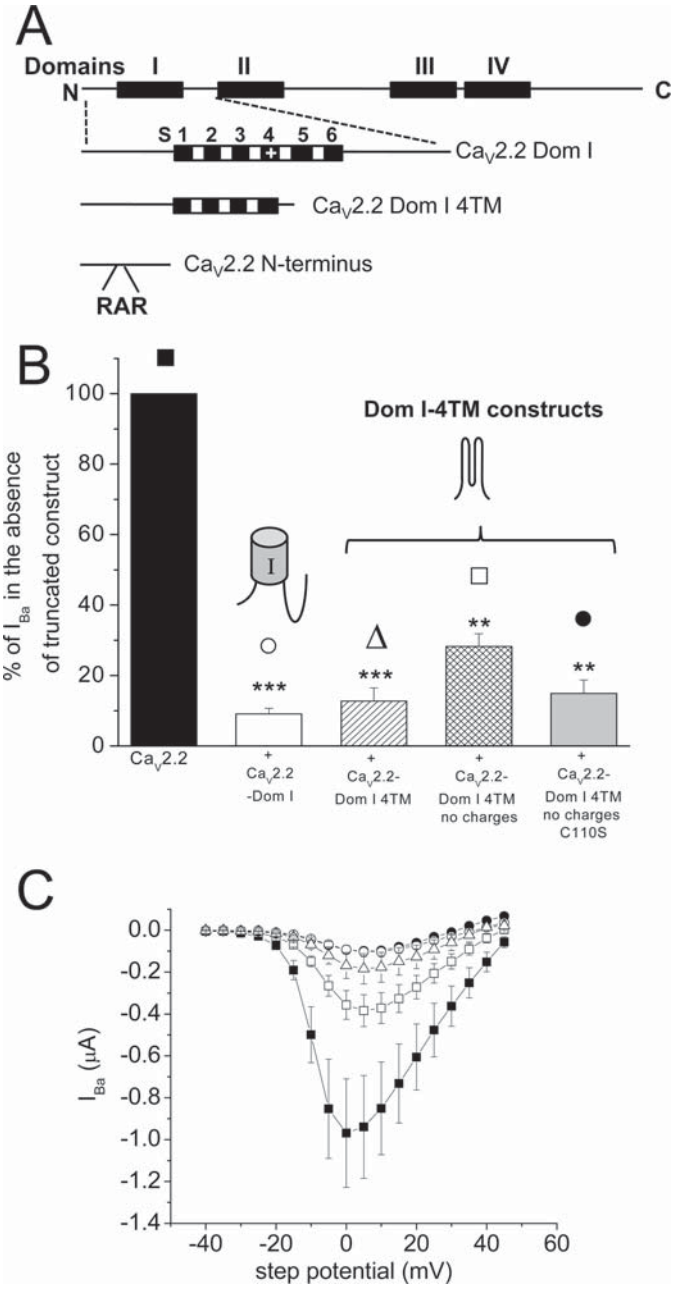

FIGURE 1. **Effect of $Ca_V2.2$-truncated domains on $Ca_V2.2$ I_{Ba} when expressed in *Xenopus* oocytes.** *A*, diagram of the main $Ca_V2.2$ constructs used in this study, as described under "Experimental Procedures." *B*, peak I_{Ba} for $Ca_V2.2/\alpha_2\delta$-2/β1b expressed in *Xenopus* oocytes without any truncated domains (*black bar*, 100%) or with $Ca_V2.2$-Dom I (*white bar*, $n = 12$; ***, $p < 0.001$), $Ca_V2.2$-Dom I-4TMs (*hatched bar*, $n = 17$; ***, $p < 0.001$), $Ca_V2.2$-Dom I-4TMs no charges (*cross-hatched bar*, $n = 14$; **, $p < 0.01$), $Ca_V2.2$-Dom I-4TMs no charges C110S (*light gray bar*, $n = 23$; **, $p < 0.01$). Data are pooled from several experiments all recorded in 5 mM Ba^{2+} and normalized to the respective control in each experiment, and the statistical differences were determined compared with their respective control data, using one-way ANOVA and Bonferroni's post hoc test. *Error bars* indicate S.E. The *symbols* above the *bars* refer to the *I-V* relationship for the representative data in *C*. *C*, mean *I-V* relationship from two pooled experiments for $Ca_V2.2/\alpha_2\delta$-2/β1b expressed in *Xenopus* oocytes without any truncated domains (■, $n = 7$) or with $Ca_V2.2$-Dom I (○, $n = 8$), $Ca_V2.2$-Dom I 4TMs (△, $n = 4$), $Ca_V2.2$-Dom I-4TMs no charges (□, $n = 11$), $Ca_V2.2$-Dom I-4TMs no charges C110S (●, $n = 7$). The *symbols* are identified above the *bars* in *B*. All recordings are in 5 mM Ba^{2+}.

We first utilized expression in tsA-201 cells and compared the ability of two N-terminally deleted, truncated constructs of $Ca_V2.2$-Dom I (Δ1–55 $Ca_V2.2$-Dom I and Δ2–91 $Ca_V2.2$-Dom

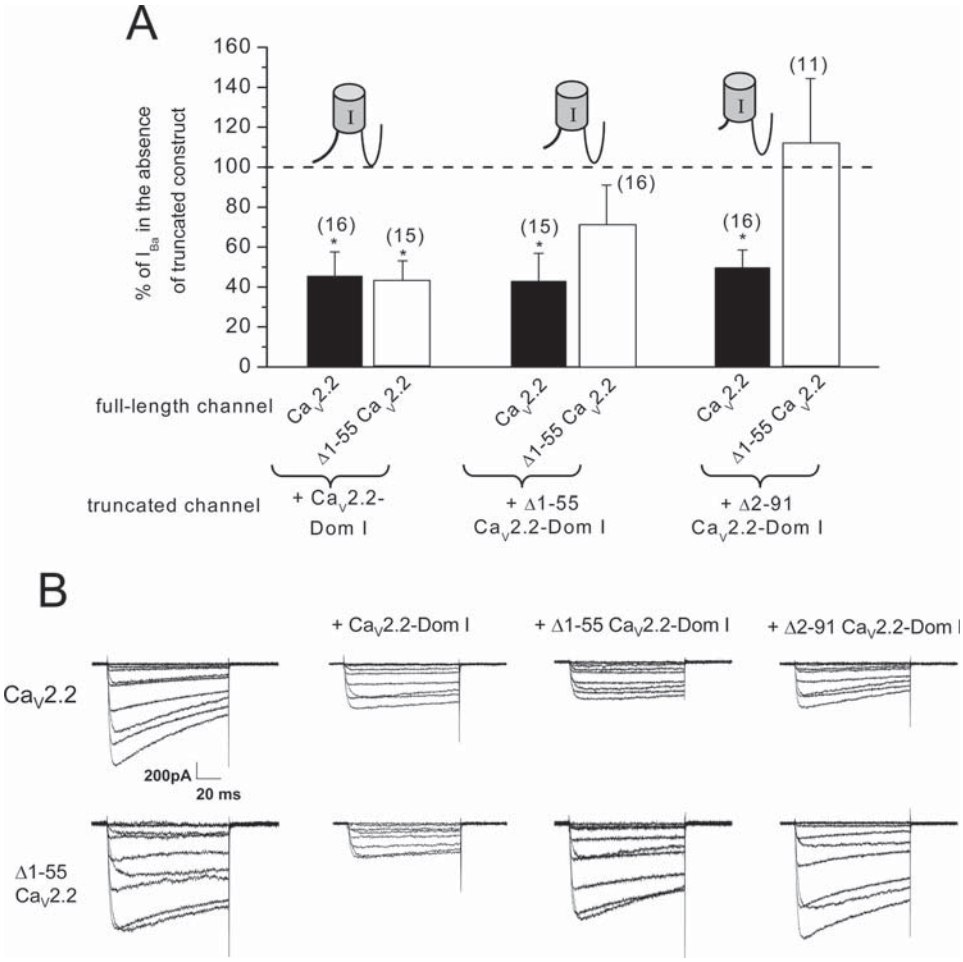

FIGURE 2. **Effect of N-terminally truncated $Ca_V2.2$ domains on $Ca_V2.2$ I_{Ba} when expressed in tsA-201 cells.** *A*, peak I_{Ba} was determined from *I-V* relationships in 1 mM Ba^{2+} following expression in tsA-201 cells. The currents in the presence of the stated truncated domain are expressed as a percentage of control currents in its absence for $Ca_V2.2/\alpha_2\delta$-2/β1b (*filled bars*) or Δ1–55 $Ca_V2.2/\alpha_2\delta$-2/β1b (*open bars*). Data were pooled from several experiments, each examining the effect of one truncated construct, and normalized to the respective control in each experiment. The statistical significances of the differences compared with control were determined by Student's *t* test; *, $p < 0.05$. The numbers of determinations are given above each *bar*. *Error bars* indicate S.E. *B*, representative current traces (from −30 to +15 mV at Δ5 mV, from a holding potential of −90 mV), for $Ca_V2.2/\alpha_2\delta$-2/β1b (*upper panel*) and Δ1–55 $Ca_V2.2/\alpha_2\delta$-2/β1b (*lower panel*) in the absence or presence of $Ca_V2.2$-Dom I, Δ1–55 $Ca_V2.2$-Dom I, or Δ2–91 $Ca_V2.2$-Dom I. The *scale bars* refer to all *traces*.

I) for their ability to suppress expression of $Ca_V2.2$ and Δ1–55 $Ca_V2.2$ I_{Ba} (Fig. 2*A*). We found that the two N-terminally truncated Domain I constructs showed consistently less suppression of Δ1–55 $Ca_V2.2$ than of $Ca_V2.2$ itself (Fig. 2), and there was no suppression of Δ1–55 $Ca_V2.2$ by the construct with the longer N-terminal deletion, Δ2–91 $Ca_V2.2$-Dom I (Fig. 2).

We then examined whether Δ2–91 $Ca_V2.2$ was functional and found that, unlike truncations up to residue 55, its expression did not result in any discernible calcium channel currents (Fig. 3*A*). We next examined whether this N-terminally truncated channel would suppress expression of the full-length WT $Ca_V2.2$ I_{Ba} and found substantial inhibition of $Ca_V2.2$ currents in *Xenopus* oocytes (Fig. 3*A*). The peak $Ca_V2.2$ I_{Ba} at +5 mV was reduced to 41.4 ± 10.1% of control ($p = 0.016$) in the additional presence of Δ2–91 $Ca_V2.2$. However, there was no effect on any other properties of the currents, including steady-state inactivation (Fig. 3*B*). A similar result was observed when the same constructs were expressed in tsA-201 cells (Fig. 3*C*). Taken together, these data suggest that at least one intact N terminus, on either the full-length or the truncated channel construct, is required for suppression; and in agreement with this hypothesis, we found no suppression of Δ1–55 $Ca_V2.2$ currents by the Δ2–91 $Ca_V2.2$ construct in the same experiment (Fig. 3*C*).

Dominant Negative Suppression Requires a Free N Terminus—To examine further the role of the N terminus, we then investigated whether its effect could be prevented by addition of a bulky tag attached to the extreme N terminus of $Ca_V2.2$. We found that there was no significant inhibition of YFP-$Ca_V2.2$ currents by YFP-$Ca_V2.2$-Dom I (14.8 ± 11.4% inhibition, Fig. 3*D*). This result indicates that the presence of an intact free N terminus, unencumbered by the bulky YFP tag, is required for dominant negative suppression.

Construct Consisting of the N Terminus of $Ca_V2.2$ Suppresses $Ca_V2.2$ Channel Expression—We had previously shown that an N-terminal construct of $Ca_V2.2$ did not inhibit GFP-$Ca_V2.2$ currents (12). This result was confirmed in the present study, the peak I_{Ba} resulting from expression of GFP-$Ca_V2.2$ was non-significantly reduced in the presence of the N terminus of $Ca_V2.2$ (residues 1–95), by 8.9 ± 19.5% ($n = 13$; Fig. 4*A*).

In the light of the results described above, we then examined whether a construct consisting of the $Ca_V2.2$ cytoplasmic N terminus alone would be capable of inhibiting WT $Ca_V2.2$ I_{Ba}. We found a 40% reduction in WT $Ca_V2.2$ currents when the $Ca_V2.2$ N terminus was co-expressed (Fig. 4, *B* and *C*).

To examine how the $Ca_V2.2$ N terminus was inhibiting $Ca_V2.2$ currents, we attached an extended CAA*X* motif to its C terminus, consisting of the last 10 amino acids of H-Ras. This would promote both prenylation and palmitoylation of the polypeptide and thus enhance the concentration associated with both plasma and internal membranes (20). To confirm the localization of constructs to which a CAA*X* motif was attached, we examined the distribution of GFP-CAA*X*, which was found to be associated both at the plasma membrane and also with cytoplasmic organelles (Fig. 4*D*), in contrast to free GFP, which was observed uniformly throughout the cytoplasm and also in the nucleus (Fig. 4*D*). The membrane-tethered $Ca_V2.2$ N terminus-CAA*X* produced a very strong inhibition of $Ca_V2.2$ currents, by 70% at 0 mV, whereas a control prenylated protein (GFP-CAA*X*) produced no significant inhibition (Fig. 4, *B*, *C*, and *E*).

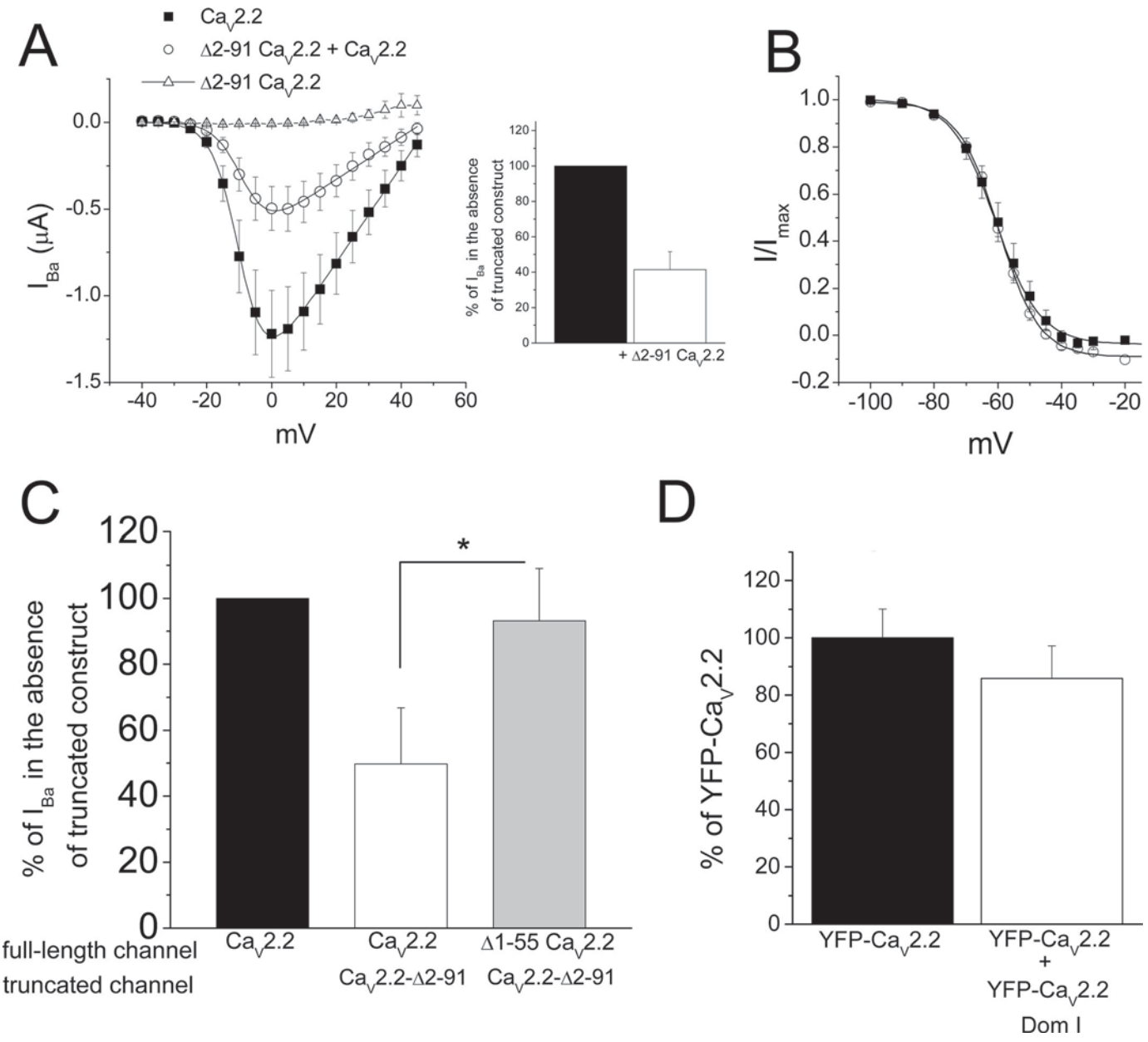

FIGURE 3. **Effect of Δ2–91 $Ca_V2.2$ and YFP-tagged $Ca_V2.2$ on $Ca_V2.2$ I_{Ba}.** *A*, mean *I-V* relationship for $Ca_V2.2$ (■, $n = 12$) or Δ2–91 $Ca_V2.2$ (△, $n = 3$) co-expressed with $\alpha_2\delta$-2/β1b in *Xenopus* oocytes, either alone or together (○, $n = 13$). All recordings are in 10 mM Ba^{2+}. The *I-V* curves are fit with a modified Boltzmann relationship, as described under "Experimental Procedures." *Inset*, bar chart of peak I_{Ba} determined from these *I-V* relationships. The currents in the presence of Δ2–91 $Ca_V2.2$ (*open bar*, $n = 13$) are expressed as a percentage of control I_{Ba} in its absence (*black bar*), for $Ca_V2.2/\alpha_2\delta$-2/β1b. *B*, lack of effect of co-expression of $Ca_V2.2$ with Δ2–91 $Ca_V2.2$ (○, $n = 6$) on the voltage-dependence of steady-state inactivation of $Ca_V2.2/\alpha_2\delta$-2/β1b I_{Ba} (■, $n = 8$) from the same experiments as in *A*. Data are fit with a Boltzmann function, as described under "Experimental Procedures." *C*, peak I_{Ba} was determined from *I-V* relationships in 1 mM Ba^{2+} following expression of constructs in tsA-201 cells. The currents in the presence of Δ2–91 $Ca_V2.2$ are expressed as a percentage of control I_{Ba} in its absence (*black bar*), for $Ca_V2.2/\alpha_2\delta$-2/β1b (*open bar*, $n = 20$), or Δ1–55 $Ca_V2.2/\alpha_2\delta$-2/β1b (*gray bar*, $n = 16$). Data were pooled from several experiments and normalized to the respective control in each experiment. The statistical significances of the differences compared with control were determined by Student's *t* test, $p < 0.05$. *Error bars* indicate S.E. *D*, lack of effect of YFP-$Ca_V2.2$-Dom I on YFP-$Ca_V2.2$ I_{Ba} in *Xenopus* oocytes. Peak currents at +5 mV are shown for YFP-$Ca_V2.2/\alpha_2\delta$-1/β1b alone (*black bar*, $n = 24$) or plus YFP-$Ca_V2.2$-Dom I (*open bar*, $n = 20$). Data were obtained in three different experiments, all with similar results. No significant differences were observed between the conditions, $p > 0.05$, Student's *t* test.

We then examined whether truncation of the $Ca_V2.2$ N terminus would prevent this inhibition and found that no significant inhibition was produced by $Ca_V2.2$ N terminus (Δ2–42)-CAA*X* (Fig. 4*B*), indicating that the extreme N terminus is involved in the process of suppression of $Ca_V2.2$ currents. We previously identified an 11-amino acid motif (residues 45–55) in the N terminus of $Ca_V2.x$ channels, YKQS*x*AQRART, which was essential for G protein-mediated inhibition of these channels (17, 21). Two key amino acids involved in this process were found to be the two arginine residues in this motif. We therefore examined whether the same motif was involved in suppression of $Ca_V2.2$ current expression by mutating these two amino acids to alanine in the $Ca_V2.2$ N terminus-CAA*X* construct. We found that these mutations prevented the effect of the N terminus on $Ca_V2.2$ currents, even producing a small increase compared with $Ca_V2.2$ alone (Fig. 4, *B* and *E*). Together with the

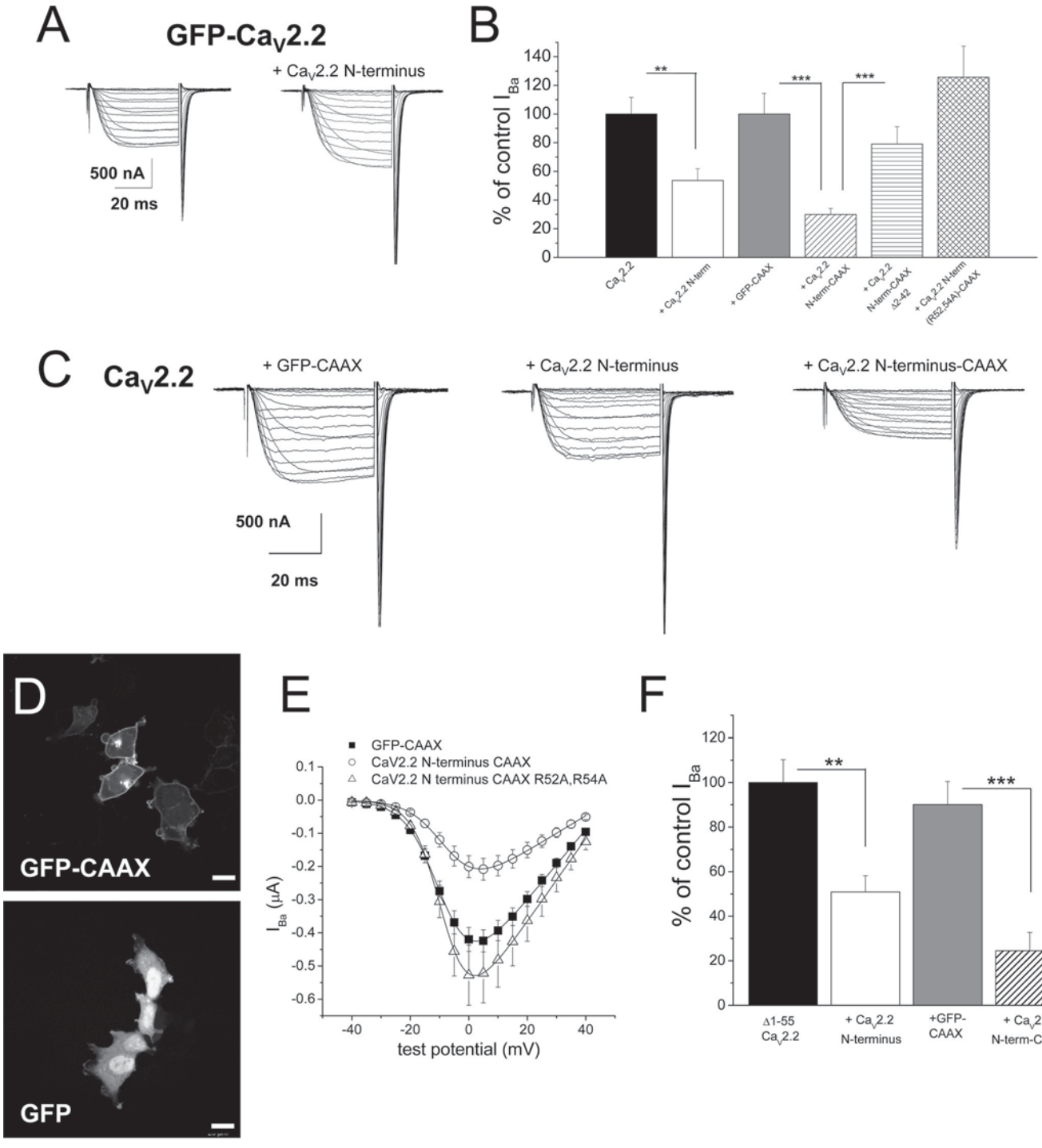

previous result, this suggests that docking of the free N terminus via a motif including Arg^{52} and Arg^{54} is involved in its ability to suppress $Ca_V2.2$ currents but that the extreme N terminus of $Ca_V2.2$ must also play a role.

Further studies showed that co-expression of the $Ca_V2.2$ N-terminal construct also produced a significant inhibition (~50%) of Δ1–55 $Ca_V2.2$ I_{Ba} (Fig. 4*F*), and co-expression of $Ca_V2.2$ N terminus-CAAX strongly inhibited (by 75%) Δ1–55 $Ca_V2.2$ I_{Ba} (Fig. 4*F*), indicating that the suppressive effect of the $Ca_V2.2$ N terminus does not require the presence of the same motif on the full-length channel. This provides evidence that the suppressive effect is probably not via dimerization of the N termini.

One potential explanation for the reduction of $Ca_V2.2$ I_{Ba} by the $Ca_V2.2$ N-terminal construct, given the involvement of the amino acids 45–55 (17, 21), was that there could be tonic modulation of the calcium channel currents (22). However, co-expression of the $Ca_V2.2$ N-terminal constructs was not associated with slowed activation of the $Ca_V2.2$ currents (Fig. 4*G*). This was therefore discarded as a possibility.

Inhibition of $Ca_V2.1$ by the N Terminus of $Ca_V2.1$—We next examined the effect of the N terminus of $Ca_V2.1$ on the expression of the P/Q-type channel $Ca_V2.1$. Co-expression of the $Ca_V2.1$ N terminus with $Ca_V2.1/\alpha_2\delta$-2/β4 produced 37.9% inhibition of the peak I_{Ba} currents (Fig. 5, *A* and *B*). The relevance of this combination of channel subunits is that it is likely to be one of the main channel complexes in cerebellar Purkinje neurons (13), which mediates many of the effects of the mutations in episodic ataxia type 2. The effect of co-expression of the N terminus of $Ca_V2.1$ attached to a CAA*X* motif was a 43.8% reduction in peak I_{Ba}, and this was also reversed by the corresponding mutations in the key arginine residues, Arg^{57} and Arg^{59} (Fig. 5*B*).

Furthermore, the CAA*X* motif-linked N terminus of $Ca_V2.2$, which has a strong homology to $Ca_V2.1$, also inhibited $Ca_V2.1$ currents by 63.5%, whereas the mutant R52A/R54A $Ca_V2.2$ N terminus-CAA*X* construct produced no inhibition, rather resulting in an increase in the peak I_{Ba} compared with $Ca_V2.1/\alpha_2\delta$-2/β4 alone (Fig. 5*C*).

Biochemical Basis for Suppression by the $Ca_V2.2$ N Terminus of $Ca_V2.2$ Channel Expression—We previously established that dominant negative suppression by truncated constructs involves a reduction of $Ca_V\alpha1$ subunit protein expression (9, 12). In the present study, we found that co-expression of the $Ca_V2.2$ N terminus-CAA*X* with $Ca_V2.2/\beta1b/\alpha_2\delta$-1 in tsA-201 cells resulted in a consistent decrease in the level of $Ca_V2.2$ protein (Fig. 6*A*). This was normalized to the total amount of protein in each sample and quantified as a 53% reduction, from six separate transfections (Fig. 6*B*). We also confirmed that expression of the housekeeping gene glyceraldehyde-3-phosphate dehydrogenase (*GAPDH*) was not altered by these manipulations (supplemental Fig. 1).

In our previous study implicating the unfolded protein response in this process, we also examined the level of co-expressed $\alpha_2\delta$ protein and found it also to be reduced (9). The level of $\alpha_2\delta$-1 was also reduced by co-expression of the $Ca_V2.2$ N terminus in the present study, by 51% ($n = 6$; Fig. 6, *A* and *B*). To confirm whether the RAR motif in the N terminus was involved in this response, we examined the effect of the R52A/R54A $Ca_V2.2$ N terminus-CAA*X* construct. In agreement with our electrophysiological results, the R52A/R54A $Ca_V2.2$ N terminus-CAA*X* construct produced no suppression of expression of $Ca_V2.2$ and $\alpha_2\delta$-1 protein (Fig. 6, *A* and *B*).

The inclusion of GFP as a marker of transfection and cell survival showed that the effect of $Ca_V2.2$ N terminus-CAA*X* was not due to a reduction in transfected cell number at the time of harvesting the cells. The proportion of GFP-positive cells present 48 h after transfection was 4.6 ± 0.5%, 5.8 ± 0.5%, and 4.9 ± 0.5% in tsA-201 cells transfected with $Ca_V2.2/\beta1b/\alpha_2\delta$-1/pMT2, $Ca_V2.2/\beta1b/\alpha_2\delta$-1/$Ca_V2.2$ N terminus-CAA*X*, and $Ca_V2.2/\beta1b/\alpha_2\delta$-1/R52A/R54A $Ca_V2.2$ N terminus-CAA*X*, respectively. These were not significantly different ($n = 3$, one-way ANOVA and Tukey's post hoc test).

Is There an Interaction between the N Terminus of $Ca_V2.2$ and Other Domains of $Ca_V2.2$?—We were unable to demonstrate any positive interactions between the N terminus of $Ca_V2.2$ and the $Ca_V2.2$ I-II loop, $Ca_V2.2$ Dom I or a number of other $Ca_V2.2$ sequences, using the yeast two-hybrid assay (supplemental data), in contrast to a previous study (22). Therefore we cannot identify a high affinity interaction of the $Ca_V2.2$ N terminus with a particular peptide domain of $Ca_V2.2$ using this system, indicating that it is perhaps more likely to interact in a complex binding pocket, made up of multiple elements.

Effect of Truncated Calcium Channels on Endogenous Calcium Channel Currents in DRG Neurons—We wished to examine whether the truncated constructs would also affect endogenous calcium channel currents, and we therefore expressed these constructs in DRG neurons using Amaxa transfection.

FIGURE 4. **Examination of the effect of the N terminus of $Ca_V2.2$ on functional expression of $Ca_V2.2$.** *A*, example of current traces for voltage steps from −40 mV to +40 mV from a holding potential of −100 mV for GFP-$Ca_V2.2/\alpha_2\delta$-1/β1b alone (*left*), and together with $Ca_V2.2$ N terminus (*right*). Recordings were made with 10 mM Ba^{2+} in *Xenopus* oocytes. *B*, peak I_{Ba} for $Ca_V2.2/\alpha_2\delta$-1/β1b alone (*black bar*, $n = 22$) or together with $Ca_V2.2$ N terminus 1–95 (*open bar*, $n = 36$), GFP-CAA*X* (*gray bar*, $n = 16$), $Ca_V2.2$ N terminus 1–95-CAA*X* (*hatched bar*, $n = 37$), $Ca_V2.2$ N terminus Δ2–42-CAA*X* (*horizontal striped bar*, $n = 25$), and R52A/R54A $Ca_V2.2$ N terminus-CAA*X* (*cross-hatched bar*, $n = 19$). The statistical significances of the differences indicated were determined by one-way ANOVA and Bonferroni's post hoc test. **, $p = 0.0016$; ***, $p < 0.001$. *Error bars* indicate S.E. *C*, example of current traces for voltage steps from −40 mV to +40 mV for $Ca_V2.2/\alpha_2\delta$-1/β1b with GFP-CAA*X* (*left*), with $Ca_V2.2$ N terminus (*center*), and with $Ca_V2.2$ N terminus-CAA*X* (*right*). Recordings were made with 10 mM Ba^{2+}. *D*, representative images showing the distribution of GFP-CAA*X* (*upper panel*) and free GFP (*lower panel*) expression in tsA-201 cells. *Scale bars*, 20 μm. *E*, mean *I-V* relationship for $Ca_V2.2/\alpha_2\delta$-1/β1b expressed in *Xenopus* oocytes, co-expressed with GFP-CAA*X* (■, $n = 18$), $Ca_V2.2$ N terminus-CAA*X* (○, $n = 18$), or R52A/R54A $Ca_V2.2$ N terminus-CAA*X* (△, $n = 19$). All recordings were performed in parallel using 10 mM Ba^{2+}. The *I-V* curves are fit with a modified Boltzmann relationship, as described under "Experimental Procedures." The $V_{50,\,act}$ was −8.6 mV for GFP-CAA*X*, −7.1 mV for $Ca_V2.2$ N terminus-CAA*X*, and −8.4 mV for R52A/R54A $Ca_V2.2$ N terminus-CAA*X*. *F*, peak I_{Ba} (at 0 mV) for Δ1–55 $Ca_V2.2/\alpha_2\delta$-1/β1b alone (*black bar*, $n = 34$) or together with $Ca_V2.2$ N terminus (*open bar*, $n = 36$), GFP-CAA*X* (*gray bar*, $n = 10$), and $Ca_V2.2$ N terminus-CAA*X* (*hatched bar*, $n = 9$). The statistical significances of the differences indicated were determined by Student's two-tailed *t* test. **, $p = 0.002$; ***, $p < 0.0001$. Recordings were made with 10 mM Ba^{2+}. *G*, voltage dependence of time constant of activation (τ_{act}): *left*, for $Ca_V2.2/\alpha_2\delta$-1/β1b without (■, $n = 12$) or with (○, $n = 7$) the free $Ca_V2.2$ N terminus; and *right*, for $Ca_V2.2/\alpha_2\delta$-1/β1b with GFP-CAA*X* (■, $n = 10$) or with the free $Ca_V2.2$ N terminus-CAA*X* (○, $n = 13$).

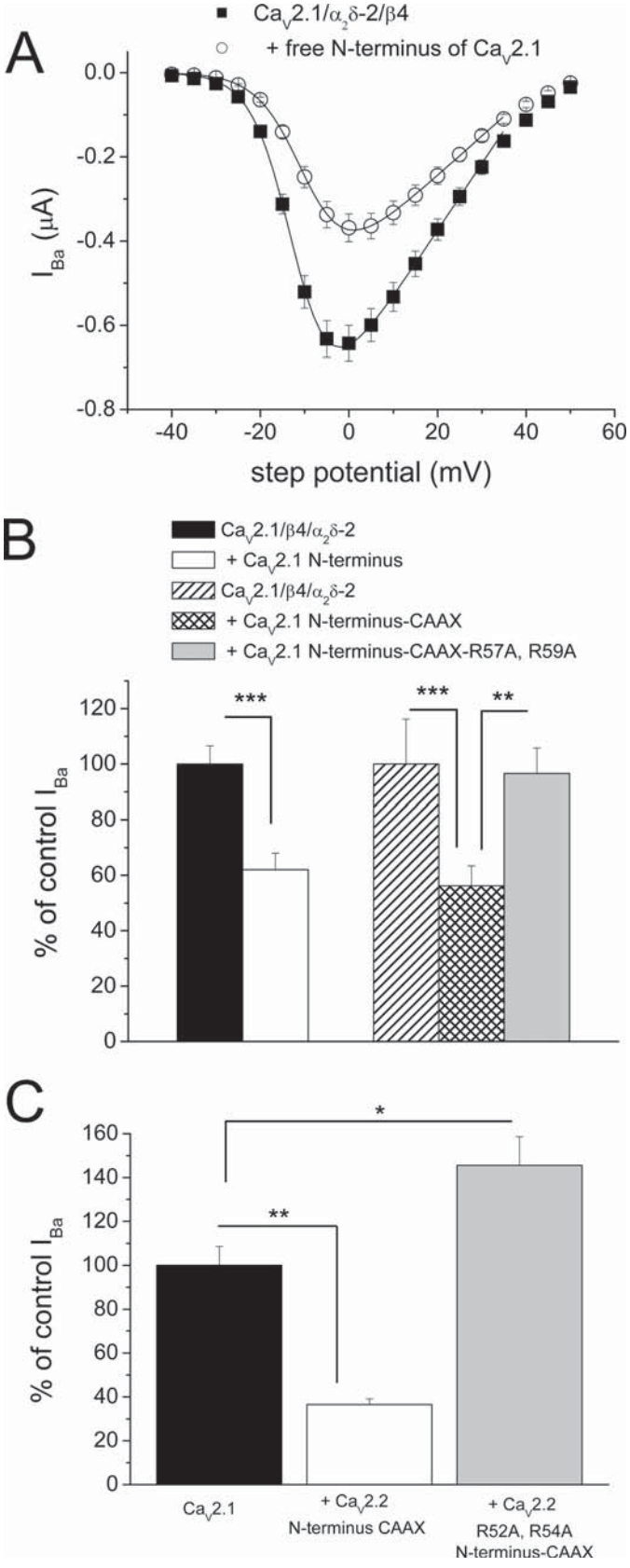

FIGURE 5. **Examination of the role of the N terminus of $Ca_V2.1$ on functional expression of $Ca_V2.1$.** *A*, mean *I-V* relationship for $Ca_V2.1/\alpha_2\delta$-2/β4 in *Xenopus* oocytes, either alone (■, $n = 15$) or co-expressed with $Ca_V2.1$ N terminus (○, $n = 15$). All recordings were performed in parallel, using 10 mM Ba^{2+}. The *I-V* curves were fit with a modified Boltzmann relationship, up to +35 mV. The $V_{50,act}$ was −11.9 mV for control and −9.3 mV in the presence of the $Ca_V2.1$ N terminus. *B*, *left panel*, peak I_{Ba} (at 0 mV) for $Ca_V2.1/\alpha_2\delta$-2/β4 alone (*black bar*, $n = 28$) or together with $Ca_V2.1$ N terminus (*open bar*, $n = 26$), from two independent experiments, including that depicted in *A*. *Right panel*, peak I_{Ba} for $Ca_V2.1/\alpha_2\delta$-2/β4 alone (*hatched bar*, $n = 9$) or together with $Ca_V2.1$ N terminus-CAA*X* (*cross-hatched bar*, $n = 20$) or $Ca_V2.1$ N terminus R57A/R59A-CAA*X* (*gray bar*, $n = 20$). The statistical significances of the differences indicated were determined by Student's two-tailed *t* test. **, $p = 0.0046$; ***, $p < 0.001$. *Error bars* indicate S.E. *C*, peak I_{Ba} (at 0 mV) for $Ca_V2.1/\alpha_2\delta$-2/β4 alone (*black bar*, $n = 23$) or together with $Ca_V2.2$ N terminus-CAA*X* (*open bar*, $n = 22$) or R52A/R54A $Ca_V2.2$ N terminus-CAA*X* (*gray bar*, $n = 22$). The statistical significances of the differences indicated were determined by ANOVA and Bonferroni's post hoc test. *, $p < 0.01$; **, $p < 0.001$.

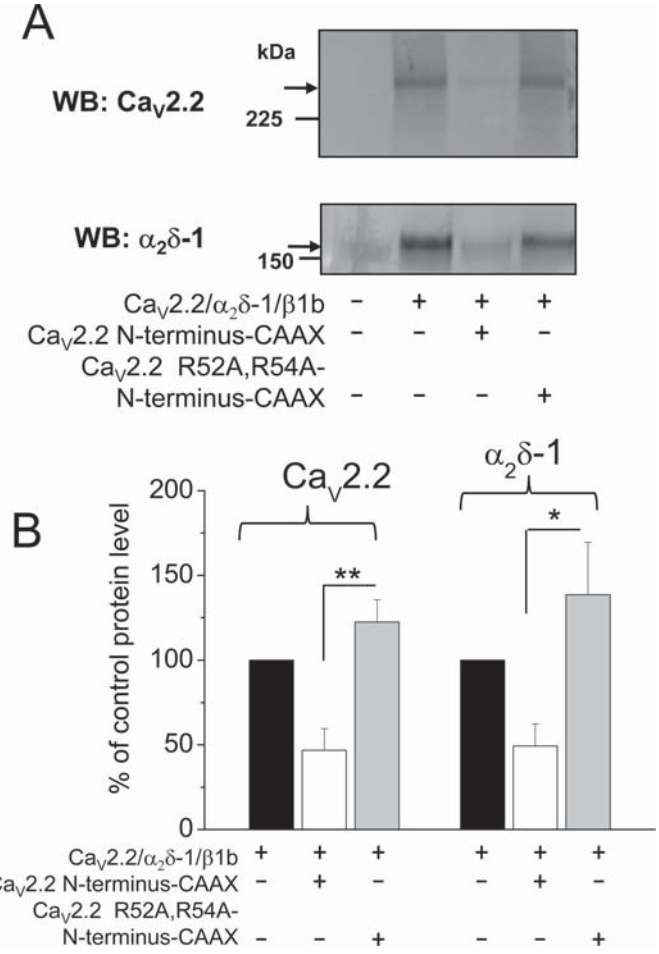

FIGURE 6. **Examination of the effect of the N terminus of $Ca_V2.2$ on $Ca_V2.2$ protein expression.** *A*, expression of $Ca_V2.2$ (*upper panel*) and $\alpha_2\delta$-1 (*lower panel*) protein in untransfected tsA-201 cells (*first lane*), when $Ca_V2.2/\alpha_2\delta$-1/β1b were expressed, alone (*second lane*) and together with $Ca_V2.2$ N terminus-CAA*X* (*third lane*), or R52A/R54A $Ca_V2.2$ N terminus-CAA*X* (*fourth lane*). The same amount of total protein was loaded for all samples on a gel, for accurate comparison among *lanes*. *B*, bar chart from quantification of results, including those in *A*, showing the effect of $Ca_V2.2$ N terminus-CAA*X* (*open bars*, $n = 6$) or R52A/R54A $Ca_V2.2$ N terminus-CAA*X* (*gray bars*, $n = 4$) relative to control levels (*black bars*), for $Ca_V2.2$ (*left*) and $\alpha_2\delta$-1 (*right*) protein levels. The statistical significance of the differences indicated were determined by Student's *t* test. *, $p = 0.0162$; **, $p = 0.0041$. *Error bars* indicate S.E.

We performed experiments 4 days after transfection, to allow synthesis of endogenous channels to occur, and in the presence of 10 μM nifedipine, to isolate native N-type calcium channel currents (Fig. 7, *A–C*). Expression of $Ca_V2.2$ N terminus-CAA*X* produced a statistically significant reduction in DRG I_{Ba} (Fig.

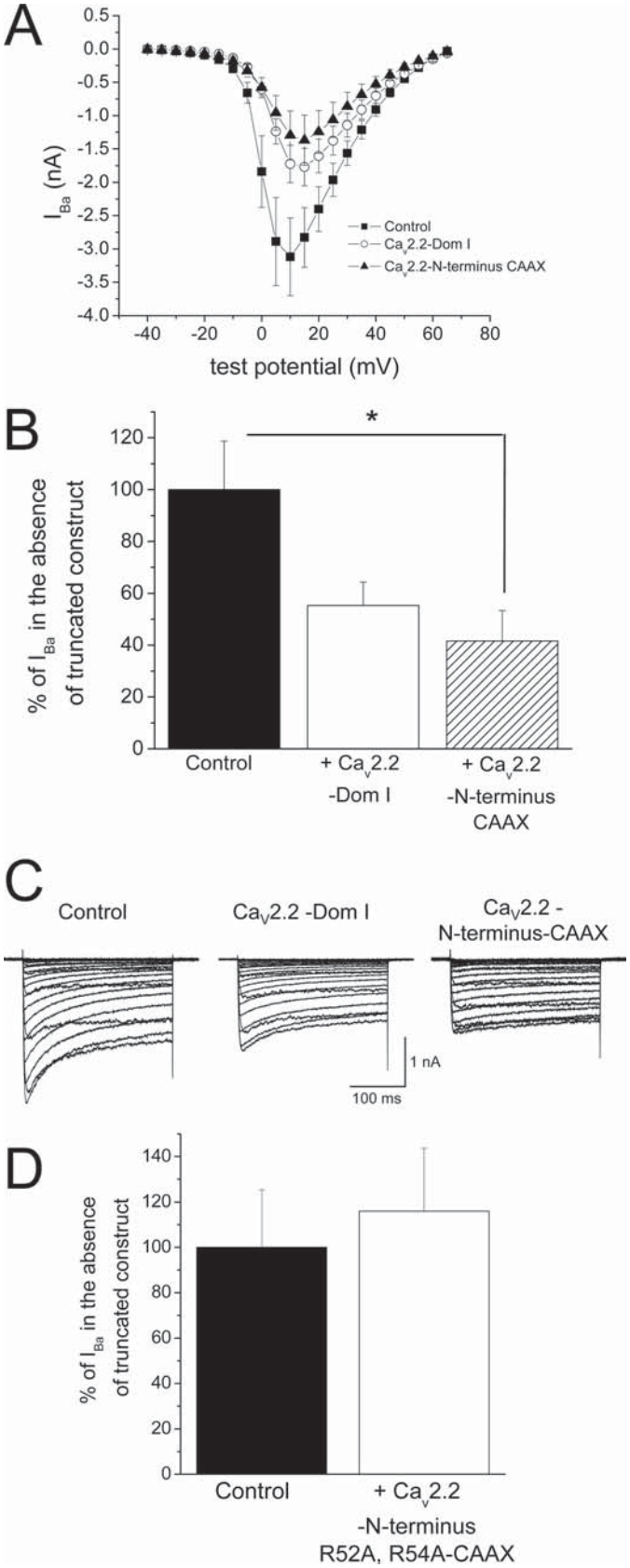

FIGURE 7. **Effect of truncated constructs containing $Ca_V2.2$ on expression of endogenous calcium channel currents in DRG neurons.** *A*, *I-V* relationship recorded in the presence of 10 μM nifedipine for DRG neurons expressing YFP (control, ■, $n = 14$), $Ca_V2.2$ Dom I (○, $n = 12$), and $Ca_V2.2$ N terminus-CAA*X*) (▲, $n = 8$). All recordings were performed 4 days after transfection. The mean ± S.E. cell capacitances were 26.4 ± 3.8, 28.4 ± 6.0, and 27.3 ± 5.5 picofarads, respectively, for the three different conditions. *B*, peak I_{Ba} (recorded in the presence of 10 μM nifedipine, at +10 mV) for DRG neurons expressing $Ca_V2.2$ Dom I (*open bar*, $n = 12$) and $Ca_V2.2$ N terminus-CAA*X*) (*hatched bar*, $n = 8$), normalized as a percentage of control (*black bar*, $n = 14$). The statistical significances of the differences were determined by one-way ANOVA followed by post-hoc Dunnett's test. *, $p < 0.05$. *Error bars* indicate S.E. *C*, example of current traces for voltage steps between −40 mV and +65 mV for neurons expressing YFP only (control) or with $Ca_V2.2$ Dom I or $Ca_V2.2$ N terminus-CAA*X* (*left* to *right*). Recordings were made with 10 mM Ba^{2+} in the presence of 10 μM nifedipine. *D*, I_{Ba} (recorded in the presence of 10 μM nifedipine at +10 mV) for DRG neurons expressing R52A/R54A $Ca_V2.2$ N terminus-CAA*X* (*white bar*, $n = 10$), normalized as a percentage of control (*black bar*, $n = 9$).

7*B*), whereas R52A/R54A $Ca_V2.2$ N terminus-CAA*X* produced no reduction in DRG I_{Ba} (Fig. 7*D*).

DISCUSSION

Here, we have examined the process of dominant negative suppression of $Ca_V2.1$ and $Ca_V2.2$ currents by truncated $Ca_V\alpha1$ constructs, which was identified by Raghib *et al.* (12). Our previous conclusion was that if $Ca_V2.2$ is co-expressed with truncated constructs of $Ca_V2.2$ containing Domain I, expression of the full-length $Ca_V2.2$ channel protein is almost completely prevented. We subsequently identified that there was a requirement for interaction between the full-length and truncated constructs (9), which has been confirmed and extended by others (10).

We previously observed cross-suppression between the different subclasses of Ca_V2 channels ($Ca_V2.1$, 2.2, 2.3), where conservation both within the TM segments and in the cytoplasmic N and C termini and loops is fairly high. However, there was no significant cross-suppression between full-length $Ca_V3.1$ and truncated constructs of $Ca_V2.2$, and vice versa (9). This suggests that the response is induced by the association of part of the truncated domain with segments of a cognate full-length channel with which it shows an affinity. Our present results identify specific motifs involved in the interaction.

We have found that one of the main regions involved in interaction is the N terminus of these channels. We observed that the optimum requirements for this to occur are that the N terminus should be both full-length and have a free N terminus (*i.e.* not tagged with XFP). When these conditions are met, in either or both of the truncated and the full-length $Ca_V2.2$ channels, suppression occurs, but when the extreme N terminus is missing from both constructs, or both are tagged with XFP, suppression is markedly reduced or absent.

Our finding that an N-terminal XFP tag hinders the dominant negative suppression process may also explain some anomalies in the literature, where such tagged constructs have been used in the study of this phenomenon (7, 23).

Amino acids 1–55 of $Ca_V2.2$ contain the N-terminal motif MVRFGDEL attached to a highly flexible region GGRYGGTGGGERARGGGAGGAGGPGQGGLPPG, representing amino acids 9–40 and identified as being glycine-rich (56%) and hence of low complexity. This region is followed by YKQSIAQRART, which is the 11-amino acid motif that we have previously identified to be essential for G protein modulation in $Ca_V2.x$ channels. This motif is highly conserved in the Ca_V2 family (17, 21) and predicted to form an α-helix (PSIPRED 2.6). An additional

motif residing within amino acids 56–95 (MALYNPIPVKQNCFTVNRSLFVFSEDNVVRKYAKRITEWPPFE) was also identified as being involved in the role of the N terminus of $Ca_V2.2$ to mediate G protein modulation by $G\beta\gamma$ (22). We have now found that this region is essential for functional expression of the channel.

A possible scenario is that the high mobility of the low complexity region in the N terminus will allow the N terminus to interact with a distant binding pocket on the channel and that the motif containing the key amino acids Arg^{52} and Arg^{54} is involved in this process. This intramolecular interaction might be required as a quality check point for correct folding during channel synthesis. *RXR* motifs have previously been identified to regulate endoplasmic reticulum retention and retrieval in other channels (24) and may be acting by a similar mechanism here.

In agreement with this hypothesis, our results show that the $Ca_V2.x$ N terminus, particularly when attached C-terminally to a CAA*X* motif, results in strong suppression of $Ca_V2.2$ expression, both in terms of functional currents and at the level of $Ca_V2.2$ protein. This suppression by the N terminus is prevented when the N terminus is truncated and when the amino acids Arg^{52} and Arg^{54} are mutated to Ala. We hypothesize that once the N terminus, either as a free domain or attached to a truncated channel, has interacted intermolecularly with the full-length channel, the misfolded aggregate may both be directed to the proteasomal pathway as suggested by others (10, 25) and may also trigger the unfolded protein response to suppress further translation (9, 26).

The relevance to episodic ataxia type 2 is that many of the mutations found in this dominant disease result in premature protein truncation, but in all the mutations to date, the N terminus is intact, the first known mutation being in Domain I (6). A number of studies have shown previously that the truncated channels predicted by episodic ataxia type 2 mutations interact with the full-length channel (9–11, 23). Here, we have identified that an intact N terminus is essential for interaction between the truncated domain and the full-length channel. Future work to discover the site of interaction may now allow the development of therapeutic agents that hinder this process.

REFERENCES

1. Catterall, W. A. (2000) *Annu. Rev. Cell Dev. Biol.* **16,** 521–555
2. Ertel, E. A., Campbell, K. P., Harpold, M. M., Hofmann, F., Mori, Y., Perez-Reyes, E., Schwartz, A., Snutch, T. P., Tanabe, T., Birnbaumer, L., Tsien, R. W., and Catterall, W. A. (2000) *Neuron* **25,** 533–535
3. Pietrobon, D. (2002) *Mol. Neurobiol.* **25,** 31–50
4. Ophoff, R. A., Terwindt, G. M., Vergouwe, M. N., van Eijk, R., Oefner, P. J., Hoffman, S. M., Lamerdin, J. E., Mohrenweiser, H. W., Bulman, D. E., Ferrari, M., Haan, J., Lindhout, D., van Ommen, G. J., Hofker, M. H., Ferrari, M. D., and Frants, R. R. (1996) *Cell* **87,** 543–552
5. Denier, C., Ducros, A., Vahedi, K., Joutel, A., Thierry, P., Ritz, A., Castelnovo, G., Deonna, T., Gérard, P., Devoize, J. L., Gayou, A., Perrouty, B., Soisson, T., Autret, A., Warter, J. M., Vighetto, A., Van Bogaert, P., Alamowitch, S., Roullet, E., and Tournier-Lasserve, E. (1999) *Neurology* **52,** 1816–1821
6. Jen, J. C., Graves, T. D., Hess, E. J., Hanna, M. G., Griggs, R. C., and Baloh, R. W. (2007) *Brain* **130,** 2484–2493
7. Wappl, E., Koschak, A., Poteser, M., Sinnegger, M. J., Walter, D., Eberhart, A., Groschner, K., Glossmann, H., Kraus, R. L., Grabner, M., and Striessnig, J. (2002) *J. Biol. Chem.* **277,** 6960–6966
8. Maquat, L. E. (2002) *Curr. Biol.* **12,** R196–R197
9. Page, K. M., Heblich, F., Davies, A., Butcher, A. J., Leroy, J., Bertaso, F., Pratt, W. S., and Dolphin, A. C. (2004) *J. Neurosci.* **24,** 5400–5409
10. Mezghrani, A., Monteil, A., Watschinger, K., Sinnegger-Brauns, M. J., Barrère, C., Bourinet, E., Nargeot, J., Striessnig, J., and Lory, P. (2008) *J. Neurosci.* **28,** 4501–4511
11. Jeng, C. J., Chen, Y. T., Chen, Y. W., and Tang, C. Y. (2006) *Am. J. Physiol. Cell Physiol.* **290,** C1209–C1220
12. Raghib, A., Bertaso, F., Davies, A., Page, K. M., Meir, A., Bogdanov, Y., and Dolphin, A. C. (2001) *J. Neurosci.* **21,** 8495–8504
13. Barclay, J., Balaguero, N., Mione, M., Ackerman, S. L., Letts, V. A., Brodbeck, J., Cantí, C., Meir, A., Page, K. M., Kusumi, K., Perez-Reyes, E., Lander, E. S., Frankel, W. N., Gardiner, R. M., Dolphin, A. C., and Rees, M. (2001) *J. Neurosci.* **21,** 6095–6104
14. Tomlinson, W. J., Stea, A., Bourinet, E., Charnet, P., Nargeot, J., and Snutch, T. P. (1993) *Neuropharmacology* **32,** 1117–1126
15. Tinker, A., Jan, Y. N., and Jan, L. Y. (1996) *Cell* **87,** 857–868
16. Cormack, B. P., Valdivia, R. H., and Falkow, S. (1996) *Gene* **173,** 33–38
17. Cantí, C., Page, K. M., Stephens, G. J., and Dolphin, A. C. (1999) *J. Neurosci.* **19,** 6855–6864
18. Campbell, V., Berrow, N., Brickley, K., Page, K., Wade, R., and Dolphin, A. C. (1995) *FEBS Lett.* **370,** 135–140
19. Cantí, C., Davies, A., Berrow, N. S., Butcher, A. J., Page, K. M., and Dolphin, A. C. (2001) *Biophys. J.* **81,** 1439–1451
20. Choy, E., Chiu, V. K., Silletti, J., Feoktistov, M., Morimoto, T., Michaelson, D., Ivanov, I. E., and Philips, M. R. (1999) *Cell* **98,** 69–80
21. Page, K. M., Cantí, C., Stephens, G. J., Berrow, N. S., and Dolphin, A. C. (1998) *J. Neurosci.* **18,** 4815–4824
22. Agler, H. L., Evans, J., Tay, L. H., Anderson, M. J., Colecraft, H. M., and Yue, D. T. (2005) *Neuron* **46,** 891–904
23. Jeng, C. J., Sun, M. C., Chen, Y. W., and Tang, C. Y. (2008) *J. Cell. Physiol.* **214,** 422–433
24. Schwappach, B., Zerangue, N., Jan, Y. N., and Jan, L. Y. (2000) *Neuron* **26,** 155–167
25. Chevet, E., Cameron, P. H., Pelletier, M. F., Thomas, D. Y., and Bergeron, J. J. M. (2001) *Curr. Opin. Struct. Biol.* **11,** 120–124
26. Ron, D. (2002) *J. Clin. Invest.* **110,** 1383–1388